MOLECULAR AND CELLULAR BIOLOGY, Feb. 2002, p. 1203–1217 Vol. 22, No. 4
0270-7306/02/$04.00+0 DOI: 10.1128/MCB.22.4.1203–1217.2002
Copyright © 2002, American Society for Microbiology. All Rights Reserved.

Focal Adhesions Require Catalytic Activity of Src Family Kinases To Mediate Integrin-Matrix Adhesion

Leiming Li,[1,2] Masaya Okura,[1]† and Akira Imamoto[1,2,3]*

The Ben May Institute for Cancer Research and Center for Molecular Oncology,[1] Committee on Cell Physiology,[2] and Committee on Cancer Biology,[3] The University of Chicago, Chicago, Illinois 60637

Received 9 July 2001/Returned for modification 17 August 2001/Accepted 20 November 2001

Members of the Src family of tyrosine kinases function to phosphorylate focal adhesion (FA) proteins. To explore the overlapping functions of Src kinases, we have targeted Csk, a negative regulator of the Src family, to FA structures. Expression of FA-targeted Csk (FA-Csk) effectively reduced the active form (nonphosphorylated at the C-terminal regulatory tyrosine) of Src members in the cell. We found that fibroblasts expressing FA-Csk lost integrin-mediated adhesion. Activated Src (SrcY529F) as well as activation of putative Src signaling mediators (Fak, Cas, Crk/CrkL, C3G, and Rap1) blocked the effect of FA-Csk in a manner dependent on Rap1. SrcY529F also inhibited activated Ras-induced cell detachment but failed to rescue detachment caused by an activated mutant of Raf1 (Raf-BXB) that Rap1 cannot inhibit. Although normal spreading onto fibronectin was restored by the β_1 integrin affinity-activating antibody TS2/16 in cells expressing FA-Csk or Raf-BXB, FAs were lost in these cells. On the other hand, Rap1 activation could restore FAs in cells expressing FA-Csk. Activation of the executioner caspase, caspase 3, is essential for many forms of apoptosis. While a caspase 3 inhibitor (Z-DEVD-FMK) inhibited cell detachment triggered by activation of caspase 8, this inhibitor had no effect on cell detachment caused by FA-Csk. Likewise, overexpression of an activated Akt made cells resistant to the effect of caspase 8 activation, but not to the effect of FA-Csk. It is therefore likely that the primary cause of cell rounding and detachment induced by FA-Csk involves dysfunction of FAs rather than caspase-mediated apoptosis that may result from possible loss of survival signals mediated by Src family kinases. We suggest that endogenous Src family kinases are essential for FAs through activation of Rap1 in fibroblasts.

The control of cell-extracellular matrix (ECM) adhesion is required for many physiological functions of stationary as well as motile cells in vivo (29). The integrin family of transmembrane proteins forms heterodimers that function as receptors for ECM proteins such as fibronectin. The engagement of integrins to the ECM triggers cascades of protein-protein interactions. Activation of protein tyrosine kinases (PTKs) such as Src family kinases and focal adhesion (FA) kinase (Fak) is one of the earliest events that immediately follow integrin-fibronectin engagement (39). While Src localizes to endosomal membranes in quiescent cells, Src transiently translocates to newly formed FA structures during cell spreading onto a fibronectin-coated surface (32). It has also been shown that Src and Fyn, another member of the Src family, bind to Fak at tyrosine 397 (Y397) upon autophosphorylation (53). Inhibition of cell spreading by an endogenous inhibitor of Fak, Frnk (Fak-related nonkinase), can be bypassed by co-overexpression of Src, potentially due to the ability of Src to phosphorylate downstream FA proteins such as paxillin (49). These observations have raised the hypothesis that Src family kinases play a role in integrin signaling at the FA protein complex.

Csk is a cytosolic tyrosine kinase that negatively regulates Src family kinases in vitro and in vivo by phosphorylating the regulatory tyrosine residue conserved among all members of the Src family (30, 42). This phosphorylation is one of the requirements for the intramolecular conformational change that maintains Src family kinases structurally and catalytically inactive (65). Csk localizes to FA structures when Src family kinases are activated (25). Furthermore, consistent with activation of Src family kinases upon cell adhesion to fibronectin, Csk transiently accumulates at the integrin-cytoskeletal protein complex upon fibronectin-integrin engagement (39). Csk can associate with phosphorylated FA proteins such as Fak and paxillin in vitro, thus suggesting that Csk translocation to FA structures is regulated by tyrosine phosphorylation (5, 51). Thus, activation as well as regulation of Src family kinases appears to take place at the FA complex. To address this hypothesis, we have devised fusion proteins of Csk that constitutively localize to FAs. With this approach, we provide formal evidence for the previous prediction that Src family kinases are regulated positively or negatively at FAs. Ras and its effector Raf1 have been implicated in inhibition of integrin affinity in hematopoietic cells (28). Our results demonstrate for the first time that in contrast to overexpression of oncogenic Src, which can activate Ras and Raf1, endogenous Src family kinases play an essential role in integrin adhesive function and FA structures through Rap1 in fibroblastic cells.

* Corresponding author. Mailing address: The University of Chicago, 924 E. 57th St., JFK-R316, Chicago, IL 60637. Phone: (773) 834-1258. Fax: (773) 702-4394. E-mail: aimamoto@midway.uchicago.edu.

† Present address: Department of Maxillofacial Surgery, Osaka University Dental Hospital, Suita, Japan.

MATERIALS AND METHODS

FAT constructs. FA-targeting (FAT) sequences were isolated from chicken *Fak* and mouse *paxillin*. The FAT sequence (encoding amino acids 854 to 1053) of chicken *Fak* was amplified by PCR with primers 5′-AGG GCC CAG CTG GTA AC-3′ and 5′-TTA GTG GGG CCT GGA CTG-3′ from the RCAS A FAK

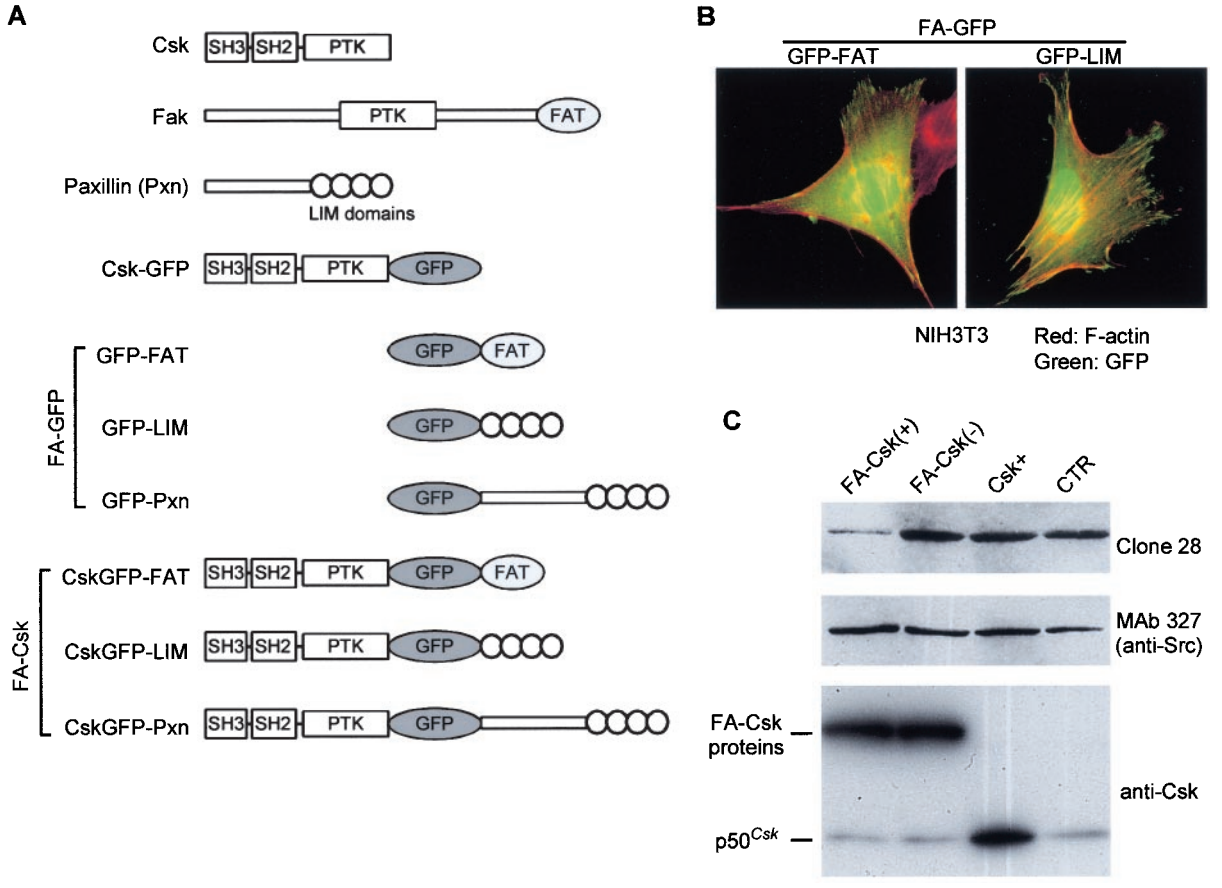

FIG. 1. Subcellular targeting of Csk to the FA complex. (A) Structures of Csk fusion proteins, Csk, Fak, and paxillin. PTK, protein tyrosine kinase domain; SH, Src homology domain; FAT, FA-targeting sequence; GFP, green fluorescent protein. The C-terminal half of paxillin contains four LIM domains. Kinase-inactive versions of Csk fusion proteins were also made with a point mutation that replaces the lysine residue (K222) at the ATP binding site with a methionine residue. (B) Subcellular localization of FA-GFP proteins (GFP-FAT and GFP-LIM) in NIH 3T3 cells was determined. Note that fusion proteins (green) are localized to FA structures at the distal tip of F-actin fibers (red). Another FA-GFP, GFP-Pxn, showed similar subcellular localization (not shown). Cells were fixed and stained with phalloidin 18 h after electroporation for transient expression of the transgene. (C) The ability of FA-targeted Csk to phosphorylate the C-terminal regulatory tyrosine of Src kinases was determined by Clone 28 immunoblot analysis. HEK 293 cells were transiently transfected by lipofection with 4 μg of kinase-active or -inactive CskGFP-FAT [FA-Csk(+) or FA-Csk(−), respectively], normal mouse Csk (Csk+), or empty vector (CTR) in a 100-mm-diameter tissue culture plate. Twenty-four hours later, cell lysates were made. Ten micrograms of total protein per lane was separated in an SDS-polyacrylamide gel and analyzed in immunoblots probed with Clone 28 (to detect Src kinases with the C-terminal tyrosine nonphosphorylated), MAb327 (to detect the total amount of Src expressed), or anti-Csk antibody (to determine the amount of transgene expression as well as endogenous Csk). All kinase-active FA-Csk constructs had similar effects on the phosphorylation status of the C-terminal tyrosine of Src kinases (not shown).

plasmid, obtained from Jeffery Hildebrand (24). cDNA fragments that encode a full-length paxillin or the LIM domains of paxillin were obtained from Sheila M. Thomas. We inserted these FAT sequences or full-length paxillin in frame into the C terminus of a modified green fluorescent protein (GFP) synthesized with the humanized codon bias (pGreenLantern-1; Life Technologies) (69). PCR-based mutagenesis was performed with *Pfu* DNA polymerase (Stratagene) to introduce mutations that increase solubility at 37°C (V163A, I167T, and S175G) in addition to the S65T mutation which had been included in the GFP sequence obtained (67). In addition to these functional modifications, we inserted a FLAG epitope and three restriction sites (each of which opens up a different reading frame) for construction of a C-terminal fusion at the N- and C-terminal ends of the GFP sequence, respectively (sequence information available upon request). pGreenLantern-1 vector is an expression vector including the human cytomegalovirus promoter and simian virus 40 polyadenylation signal. The stop codon of mouse Csk cDNA was removed by PCR-based mutagenesis using *Pfu* polymerase before insertion into the N terminus of the GFP sequence. Kinase-inactive Csk (CskK222 M) was prepared by PCR-based mutagenesis with *Pfu* polymerase. The accuracy of the mutated constructs was confirmed by DNA sequencing. These sequences were assembled as illustrated in Fig. 1.

Other expression constructs. Mouse Src cDNA fragments (normal nonneuronal Src, SrcY529F, and SrcK297M/Y529F) were inserted into a plasmid vector that contains the RNA polymerase II (Pol2) promoter and the bovine growth hormone polyadenylation signal. Similar constructs were made with pcDNA3 containing the cytomegalovirus promoter and the bovine growth hormone polyadenylation signal (Invitrogen). Mouse nonneuronal Src cDNA was obtained from Tony Hunter. SrcY529F mutant cDNA was prepared by PCR-based mutagenesis with *Pfu* polymerase. The accuracy of mutated cDNA constructs was confirmed by DNA sequencing.

BCR-ABL (p210) retroviral vector is a gift from Warren Pear. Expression plasmids for dominant negative Ras (Ras 17N in pEXV vector) and Rap1b mutants (Rap1b 17N and Rap1b 12V in pcDNA3 vector) are gifts from Alan Hall and Philip J. S. Stork, respectively. Activated mutants of H-Ras and Raf1 (Ras 61L and Raf-BXB, respectively) were gifts from Anning Lin (7, 38) and were subcloned into the bicistronic viral expression vector MIGR1 (a gift from Warren Pear [45]) designed to coexpress GFP. Activated R-Ras (R-Ras 38V) was a gift from Erkki Ruoslahti (68) and was subcloned into pcDNA3. A dominant negative Raf1 (Raf-C4) is a gift from Marsha R. Rosner (7). An expression vector for the activated p110 subunit of PI3K (Myc-tagged and membrane-

anchored, p110α-CAAX) is a gift from Julian Downward (62). Activated Akt (a fusion of Akt to the SH4 domain of Src, i.e., myristoylated Akt) in the pBABE puro retroviral vector is a gift from Suzanne Conzen (41). NIH 3T3 cells that overexpress myristoylated Akt were generated by retrovirus infection with the plasmid mentioned above.

Expression plasmids for CD2Fak and CD2Fak-Y397F are gifts from Kristina Vuori (61). Various expression plasmids for Cas and its fragments are gifts from Amy Bouton (9). Human CRKL cDNA (in pcDNA3) is a gift from Brian J. Druker. Mouse Crk II cDNA was obtained from Beatrice Knudsen and subcloned into pcDNA3. Human C3G and DOCK180 expression vectors (in pCAGGS) are gifts from Michiyuki Matsuda (22). pCEFL-CD8-C is an expression vector for a chimeric fusion protein between the CD8 extracellular-transmembrane domains and the caspase domain of caspase 8 (without the prodomain) (37).

Cells, tissue culture, and transfection. Mouse embryonic fibroblasts (MEFs) NIH 3T3, human embryonic lung fibroblasts WI-38, and human embryonic kidney 293 (HEK 293) epithelial cells were obtained from American Type Culture Collection (ATCC). MEFs that express SrcY529F were prepared by permanent transfection of *Src*$^-$ spontaneously immortalized cells with the Pol2 promoter/bpA cassette transducing SrcY529F. Cells were maintained in Dulbecco's modified essential medium (DMEM) supplemented with 10% calf serum.

For transient expression, we used electroporation or Lipofectamine reagent (Life Technologies) with uncut plasmids. Electroporation was carried out with 20 μg of plasmid for 10^7 cells at 280 V and 500 μF. Cells were plated onto a glass coverslip coated with an ECM protein for subsequent observation of GFP and cell staining. In dose-response experiments with multiple plasmids using Lipofectamine reagent, we adjusted the combined amount of plasmids to 0.2 or 0.4 μg/well in a 24-well plate by adding an empty plasmid in order to use the same ratio and amount of DNA and reagent in each group. For biochemical analysis, cells were transfected in a 60-mm-diameter tissue culture plate. We used the conditions for transfection with Lipofectamine reagent described in the manufacturer's protocol. After 3 h of lipofection in serum-free DMEM or electroporation, cells were cultured in the presence of 10% calf serum unless otherwise stated for the period indicated in the appropriate figure legend before examination.

Cell staining. After transfection (18 or 24 h after electroporation or Lipofectamine treatment, respectively), cells were fixed by buffered formalin solution at room temperature for 5 min. Fixed cells were permeabilized with 0.1% Triton X-100 in phosphate-buffered saline (PBS) and blocked with bovine serum albumin and normal goat serum. Cells were incubated with the following primary antibodies: anti-Csk rabbit polyclonal antibody (Santa Cruz), anti-Fak rabbit polyclonal antibody against the N-terminal peptide (Santa Cruz Biotechnology), antipaxillin mouse monoclonal antibody (Transduction Laboratories), antivinculin mouse monoclonal antibody (Sigma), or anti-mouse Enabled rabbit polyclonal antibody (a gift from F. B. Gertler [20]). We found that the epitope of the antipaxillin antibody is outside the LIM domains. Alexa 594-conjugated secondary goat antibodies (Molecular Probes) were used to detect the staining. To observe the actin cytoskeleton, Alexa 594-conjugated phalloidin (Molecular Probes) was used. When necessary, the nucleus was counterstained with 4′,6′-diamidino-2-phenylindole (DAPI) (Molecular Probes). After staining, cells were mounted in Prolong antifade reagent (Molecular Probes). Cellular staining was observed in an Axiovert microscope equipped with fluorescent attachment and filter combinations for DAPI, red-shifted GFP, and Texas Red (compatible with Alexa 594). Photomicrographs were recorded by a cooled charge-coupled device camera controlled by an O2 Workstation (Silicon Graphics).

Quantitation of fluorescent images. Levels of immunostained proteins were quantitatively measured by NIH Image software (developed at the National Institutes of Health and available on the Internet at http://rsb.info.nih.gov/nih-image/) as previously described (23). To assess the total value of signal intensity in the cell, the mean pixel density was multiplied by the number of pixels in the cell. Original digital images (without gamma adjustment in TIFF format) that included both transfected and nontransfected cells were chosen. The ratio of the total value of intensity of transfected cells to the total value of intensity of nontransfected cells was calculated for each image. The final data were obtained by averaging the ratios of multiple images.

Rescue experiments with β_1 integrin-activating antibody. WI-38 human lung fibroblasts were transfected by electroporation with CskGFP-FAT (kinase active or inactive), activated Raf1 (Raf-BXB), or empty control vector and plated on a nontissue culture petri dish coated with poly-L-lysine (PLL) in order to prevent cell detachment that may be caused by FA-Csk(+) or Raf1-BXB expression. In experiments with Raf1-BXB, WI38 cells were cotransfected with GFP-LIM or GFP-PXN to assess FAs. Cells were cultured for 16 h in DMEM supplemented with 10% fetal bovine serum to allow efficient expression of the transgene. After this period, cells were washed with PBS and incubated with 2 μg of cycloheximide per ml in serum-free DMEM for 2 h to prevent production of ECM proteins by these cells. Cells were then trypsinized and treated with soybean trypsin inhibitor (Sigma). Cells were preincubated with the human β_1-activating monoclonal antibody TS2/16 at 37°C in serum-free DMEM in suspension for 30 min. After being washed, cells were plated onto fibronectin-coated coverslips. Cells with phase-refractive spherical morphology were scored as nonspreading, whereas those with extended cellular processes were scored as spreading. Cell spreading was evaluated as the percentage of spreading cells to total cells for each field. The number of GFP-positive cells spread at 1 h was determined. The total number of GFP-positive cells that remained attached was also determined. Since FAs in WI38 cells were more distinct at 2 h than 1 h after replating, some cells were cultured for 2 h after replating with or without TS2/16 pretreatment for observations of FAs and cell morphology. The TS2/16.2.1 hybridoma cell line was obtained from ATCC.

Time-lapse observations. Normal MEFs (10^7 cells) were electroporated with FA-Csk vectors and seeded onto a glass surface coated with fibronectin. The coverslip was assembled into a thin temperature-controlled chamber (FCS2; Bioptechs, Inc.) that allows continuous flow of fresh tissue culture media during observation under an Axiovert microscope (Carl Zeiss). Time-lapse photomicrographs were taken with a cooled charge-coupled device camera controlled by an O2 Workstation (Silicon Graphics).

Immunoblotting analysis. Cell lysates were prepared in radioimmunoprecipitation assay buffer containing 1 mM sodium orthovanadate, 15 μg of aprotinin per ml, 1 μg of leupeptin per ml, and 0.1 mM phenylmethylsulfonyl fluoride. Sodium dodecyl sulfate-polyacrylamide gel electrophoresis and immunoblot analysis were performed according to a standard protocol. Monoclonal anti-Src antibody 327 (MAb327; a gift from Joan Brugge) was used to detect Src expression. Clone 28 (a gift from Hisaaki Kawakatsu and Koji Owada) is a monoclonal antibody that recognizes the nonphosphorylated status of the Csk target site (Y529 or Y531 in mouse or human Src, respectively) conserved among the members of the Src family (35). Polyclonal anti-Csk antibody (Santa Cruz) was used to compare the level of FA-Csk expression with the level of endogenous Csk. Anti-DOCK180 and anti-Akt1/2 polyclonal antibodies were obtained from Santa Cruz Biotechnology, and anti-p110α monoclonal antibody was obtained from BD Transduction Laboratories. After incubation with peroxidase-conjugated secondary antibodies (Jackson Immunolab), blots were developed with a chemiluminescent agent (Pierce). The results of each immunoblot were analyzed by the NIH Image program for quantitation with at least two different exposures to avoid over- or underexposure.

Caspase inhibitor treatment. After transfection, cells were incubated with or without the caspase 3 inhibitor Z-DEVD-FMK (Calbiochem) in DMEM supplemented with 10% calf serum.

Terminal deoxynucleotidyltransferase-mediated dUTP-biotin nick end labeling (TUNEL). To prevent cell detachment caused by FA-Csk while enhancing formation of FAs, glass coverslips were sequentially coated with PLL and fibronectin with a method previously described (48). After plating (in a 24-well plate with the coated coverslips), NIH 3T3 cells were cultured overnight in DMEM containing 10% calf serum and transfected in serum-free DMEM containing an expression vector by the lipofection method described above. After 3 h, transfection medium was replaced with DMEM containing 10% calf serum. After 18 h, cells were fixed with neutral buffered formalin for 5 min at room temperature. Cells were permeabilized with 0.01% Triton X-100. To block endogenous biotinylated proteins, coverslips were incubated with streptavidin and subsequently with an excess amount of biotin (to block the remaining biotin-binding sites of the streptavidin) by using a kit available from Molecular Probes. After blocking, cells were incubated with biotinylated-14-dATP (Roche) and terminal deoxynucleotide transferase (TdT; obtained from Roche) in 30 mM Tris (pH 7.2)–140 mM sodium cacodylate–1 mM $CoCl_2$ (TdT buffer). Positive controls for the TdT reaction were prepared by brief treatment of cells with DNase I (5 min) prior to the TdT reaction. After the TdT reaction, cells were washed with PBS and nick end labeling was detected by incubation with mouse anti-biotin monoclonal antibody (Jackson Immunolab) followed by Alexa 594-conjugated anti-mouse immunoglobulin G (IgG) (Molecular Probes).

RESULTS

Subcellular targeting of Csk to FAs. It has been reported that Src is localized to FAs in *Csk*$^-$ cells, and that introduction of kinase-inactive Csk into these cells results in colocalization of Src and Csk, thus suggesting that the FA complex may be

the major site for Src regulation (25). To test this hypothesis, we have engineered mutant Csk proteins that constitutively localize to the focal adhesion (FA) complex. It has been shown that Csk can associate with at least two FA proteins, Fak and paxillin (5, 51). These proteins contain FA-targeting sequences known as FAT and LIM domains, respectively (6, 24). We took advantage of these FA-targeting sequences as well as a full-length paxillin sequence to construct Csk fusion proteins as illustrated in Fig. 1A. Subcellular targeting to the FA complex by fusion of GFP and FA-targeting sequences was successful and did not cause notable morphological changes (Fig. 1B).

In order to determine the phosphorylation status of the C-terminal regulatory tyrosine (the Csk target site) of Src members, we used Clone 28 monoclonal antibody to detect the nonphosphorylated regulatory tyrosine (thus in the active state) by immunoblot analysis of lysates of HEK 293 cells transfected with Csk transgenes. The amino acid sequence at the C terminus of Src (TEPQY*QPGENL, where Y* is the Csk phosphorylation site) is highly conserved among all members of the Src family (in fact, it is identical for Src, Fyn, and Yes). Therefore, Clone 28 recognizes most members of the Src family when the C-terminal tyrosine is not phosphorylated. We found that transient expression of kinase-active versions of FA-targeted Csk [FA-Csk(+)] dramatically reduced the active status of Src members whereas overexpression (approximately five- to sixfold the level of endogenous Csk) of normal mouse Csk or kinase-inactive FA-Csk [FA-Csk(−)] did not cause a significant change (Fig. 1C). After normalization with the total amount of Src detected by MAb327, we estimated that the active form of Src members in cells transfected with FA-Csk(+) was approximately 1/10 that of controls. As the transfection efficiency was approximately 90% in 293 cells, active Src members in remaining nontransfected cells (that is, ≈10% in the transfected group) may explain the residual amount of Clone 28-reactive Src members in the FA-Csk(+) group. Therefore, virtually all Src members appear to be phosphorylated at the regulatory site by FA-Csk(+). These results confirm the previous prediction that FAs are the major sites at which Src family members are dynamically (positively or negatively) regulated (25).

Loss of cell-matrix adhesion in fibroblasts expressing FA-Csk. While HEK 293 cells were relatively tolerant to transient expression of FA-Csk(+) (not shown), FA-Csk(+) induced a drastic change in NIH 3T3 cells and MEFs. As expected, kinase-inactive FA-Csk(−) proteins localized to FA structures without inducing notable differences in cell morphology or in the F-actin staining pattern when examined 18 h after electroporation. In contrast, all FA-Csk(+) constructs resulted in spherical morphology on a fibronectin-coated surface in approximately 80 to 90% of GFP-positive fibroblasts (MEFs and NIH 3T3) (Fig. 2A; results with CskGFP-Pxn not shown). Csk fusion without an FAT sequence (Csk-GFP) or fusion proteins without Csk (FA-GFPs) did not result in abnormal morphology in these cells (Fig. 1B; Csk-GFP data not shown).

We noted that the number of FA-Csk(+)-expressing cells was approximately 15% that of the control (GFP alone), suggesting possible cell loss from the fibronectin-coated surface (Fig. 2B). To determine whether FA-Csk(+) expression leads to cell detachment from a fibronectin-coated surface, we introduced FA-Csk proteins to cells that had been spread using a lipofection method. In addition, we tested different ECM proteins as well as PLL (PLL molecular weight, 30,000 to 70,000) in order to determine whether this phenotype was related to dysfunction of integrins. Consistent with this hypothesis, expression of FA-Csk(+) resulted in cell detachment from coverslips coated with fibronectin, vitronectin, or gelatin but not from PLL (Fig. 2C). We noted little difference in morphology or in the number of cells between the groups expressing FA-Csk(+) or FA-Csk(−) on PLL. Although the number of FA-Csk(+)-expressing cells attached to a non-coated glass surface was comparable to that of PLL (Fig. 2C), they showed rounding morphology instead of a flat or spread shape like those on PLL-coated coverslips (Fig. 2D). Furthermore, the incidence of cell detachment increased when the glass surface was covered by increasing concentrations of fibronectin (Fig. 2E).

The constructs we used resulted in similar expression levels of FA-Csk(+) and FA-Csk(−) as shown in Fig. 1C. The level of FA-Csk fusion proteins in individual NIH 3T3 cells ranged from 0.45 to 2.88 (average, 1.18; calculated from eight images that included 14 transfected cells and 19 nontransfected cells.) relative to the endogenous level of Csk (Fig. 2F). When lipofection was used with 0.1 μg of the expression vector per 1 well of a 24-well plate, the expression level was comparable to but slightly higher than that obtained with electroporation (data not shown). Hence, physiological levels of FA-Csk(+) were sufficient to induce the cell rounding and detachment phenotype. Furthermore, FA-Csk(−) proteins did not affect localization of Fak or paxillin to FAs under our experimental conditions (Fig. 2G; paxillin data not shown), thus suggesting that the effect of FA-Csk(+) is unlikely due to potential replacement of endogenous Fak or paxillin with FAT or LIM domains at FAs. These results suggest that the cell rounding and detachment phenotype caused by FA-Csk is due to constitutive subcellular localization of Csk catalytic activity to the FA complex.

Src activation blocks the effect of FA-Csk. To confirm that the effect of FA-Csk was due to the ability of Csk to repress Src family kinases, we examined the effect of FA-Csk on MEFs that express an activated mouse Src in which the regulatory tyrosine is replaced with a phenylalanine residue (SrcY529F). MEFs expressing SrcY529F should be resistant to FA-Csk if the cell rounding and detachment phenotype is due to loss of the activity of Src family members. To minimize overactivation of physiological or nonphysiological pathways by this constitutively active Src, we used MEFs that express SrcY529F in an *Src*$^{-}$ background at a protein expression level of approximately one-fifth that of the endogenous level of Src in wild-type cells (Fig. 3A). These MEFs showed a morphology similar to that of normal MEFs. Indeed, these cells remained spread on the fibronectin-coated surface when transfected with FA-Csk(+) (Fig. 3A). Furthermore, SrcY529F rescued the cell detachment phenotype of FA-Csk(+) in a dose-dependent manner while SrcY529F by itself led to cell detachment from a fibronectin-coated surface at the highest concentration examined (Fig. 3B). In contrast, a kinase-inactive variant of SrcY529F (Src-K297M/Y529F) could not rescue the effect of FA-Csk(+) (Fig. 3B). Interestingly, overexpression of normal Src could also rescue the cell detachment phenotype, albeit at a dose range higher than that of Src-Y529F, suggesting that abnormally high

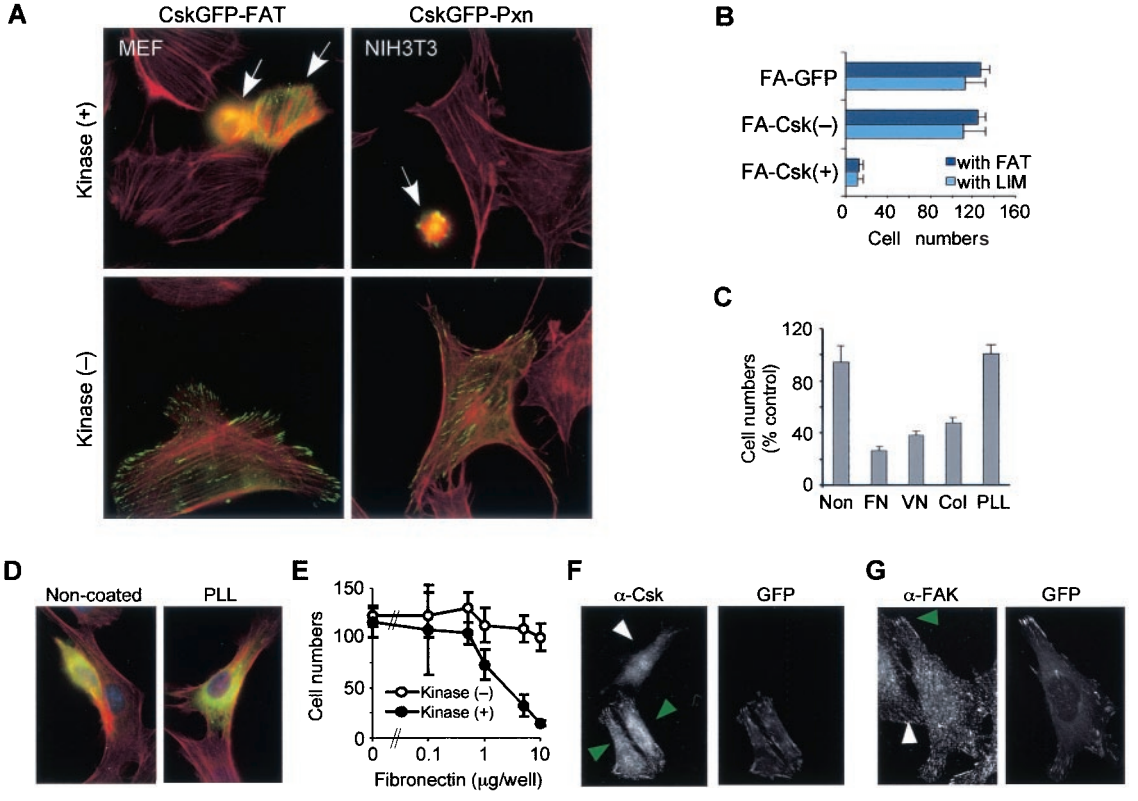

FIG. 2. Loss of integrin-mediated adhesion caused by FA-Csk. (A) The morphologies of wild-type MEFs and NIH 3T3 cells expressing kinase-active or -inactive FA-Csk constructs were determined after transient expression of the transgene. Only one example of each construct with each cell type is shown. Phalloidin staining is shown in red. Green indicates GFP fluorescence in the transfected cell (arrows). (B) The numbers of GFP-positive NIH 3T3 cells remaining on fibronectin-coated coverslips were determined in 30 random fields under a 25× objective and expressed as percentages (± standard deviations [SD] in a triplicate experiment) of the control group electroporated with GFP alone. (C) The numbers of GFP-positive NIH 3T3 cells remaining attached were determined on an ECM protein or PLL (PLL). Cells were transfected by lipofection with CskGFP-FAT. FN, fibronectin; VN, vitronectin; Col, denatured collagen (gelatin). The values indicate the numbers of GFP-positive cells relative to those of the control group transfected with the kinase-inactive variant. (D) Morphology of NIH 3T3 cells expressing the kinase-active version of CskGFP-FAT on PLL-coated glass coverslips. Green and red indicate GFP fluorescence and F-actin, respectively. (E) NIH 3T3 cells were plated on glass coverslips coated with increasing concentrations of fibronectin prior to transient transfection with 0.1 μg of CskGFP-FAT construct per well by lipofection. The *y* axis shows the total number (mean ± SD in a triplicate experiment) of GFP-positive cells remaining on the tissue culture surface in each group. (F) NIH 3T3 cells were stained with anti-Csk antibody (α-Csk) after electroporation with kinase-inactive CskGFP-FAT in order to determine expression levels of the transgene compared to endogenous Csk. Green and white arrowheads indicate cells transfected and nontransfected, respectively. Levels of proteins identified by anti-Csk antibody were measured as described in Materials and Methods. (G) NIH 3T3 cells were plated on fibronectin-coated coverslips and stained with an anti-Fak antibody (α-Fak) after electroporation with kinase-negative CskGFP-FAT. This antibody detects endogenous Fak but not the fusion protein, as it recognizes the N terminus of Fak. Green or white arrowheads indicate endogenous Fak at FA structures in a transfected cell or in a nontransfected cell, respectively. In all experiments shown (panels A to G), cells were cultured in DMEM containing 10% calf serum for 18 h after transfection before fixation. All experiments were repeated at least three times.

ratios of Src to Csk (endogenous Csk and FA-Csk) may also activate Src (Fig. 3B). Therefore, the cell rounding and detachment phenotype of FA-Csk is most likely due to its ability to repress the catalytic activity of Src family kinases efficiently at the focal complex.

The inhibitory effect of v-Src or activated Src on cell adhesion has been described previously (28). However, we noted that *Csk*$^{-}$ MEFs, in which endogenous Src family kinases are activated, adhere well to the fibronectin-coated surface although they show accumulation of FA proteins and F-actin into podosome-like large cell-matrix adhesion structures (58). The results shown in Fig. 3B also suggest that the function of Src is sensitive to the level of expression or activation. We therefore determined whether activation of endogenous Src family kinases rescues the FA-Csk phenotype. The inactive state of Src is maintained by intramolecular binding between the SH2 domain and phosphorylated Y529 (in mouse Src; equivalent to Y527 in chicken Src) as well as by association of the SH3 domain with the linker sequence between the SH2 and kinase domains (65). It has been reported that Fak and Cas can disrupt the inactive conformation of Src by their interactions with the Src SH2 and SH3 domains, respectively (9, 52). While phosphorylated Y397 of Fak is a binding site for the SH2 domains of Src and Fyn (53), the proline-rich motif at the C-terminal region of Cas binds to the SH3 domain of Src (9). In fact, expression of activated Fak (a membrane-anchored Fak; CD2Fak) (19) or a C-terminal fragment of Cas (CasCT) (9) counterbalanced the effect of FA-Csk in a dose-dependent

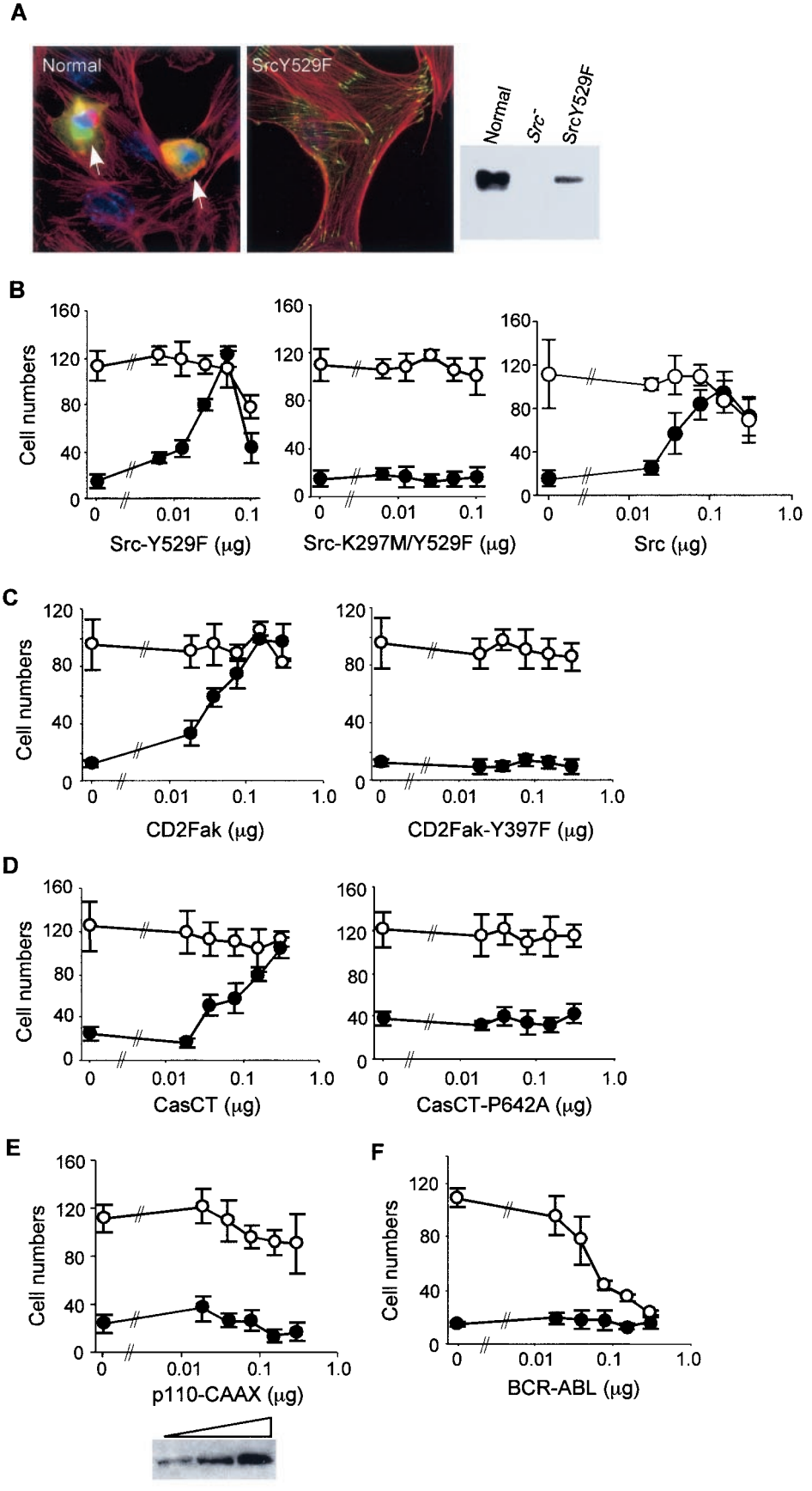
A
Normal
SrcY529F
Normal
Src-
SrcY529F
B
Cell numbers
Src-Y529F (μg)
Src-K297M/Y529F (μg)
Src (μg)
C
CD2Fak (μg)
CD2Fak-Y397F (μg)
D
CasCT (μg)
CasCT-P642A (μg)
E
p110-CAAX (μg)
F
BCR-ABL (μg)

manner whereas mutants (CD2Fak-Y397F or CasCT-P642A) incapable of binding the Src SH2 or SH3 domain failed to do so (Fig. 3C). Although the PI3K regulatory subunit p85 is also capable of binding phosphorylated Y397 of Fak (13), the fact that activated PI3K (a membrane-anchored p110α subunit, p110-CAAX) could not rescue the FA-Csk phenotype (Fig. 3D) suggests that the ability of CD2Fak to rescue the phenotype is dependent on its ability to bind Src or Fyn rather than on activation of the PI3K pathway. Therefore, consistent with the multistage Src activation-inactivation model (65), our results suggest that FA-Csk effectively shifts the balance and equilibrium of Src activation and inactivation toward inactivation at FAs.

Although another tyrosine kinase, Abl, has been implicated in mediating part of Src signaling (46), expression of p210 BCR-ABL decreased the number of cells attached to fibronectin and could not rescue the FA-Csk phenotype (Fig. 3E). Therefore, the Src family-specific tyrosine phosphorylation rather than that of Abl is required for proper cell-matrix adhesion.

Involvement of Crk/CrkL and C3G. The results shown above suggest that Src substrates may mediate cell-matrix adhesion pathways. Cas is a large adapter protein that has many protein-protein interaction domains and motifs. Src has been implicated in phosphorylation of Cas (43, 61), which then creates binding sites for other adapter proteins such as Crk (16). We found that while Crk and Crk-like (CrkL) could rescue the FA-Csk phenotype, CrkL was more effective than Crk (Fig. 4A). Unlike CrkL, however, Crk overexpression reduced the number of cells in both FA-Csk(+)- and FA-Csk(−)-transfected groups. Conversely, overexpression of dominant negative forms of CrkL induced a cell rounding phenotype in normal NIH 3T3 cells (not shown). Thus, CrkL is a candidate for mediating Src family-dependent adhesion mechanisms. One of the SH3 domains of Crk family adapter proteins associates with C3G and DOCK180, guanine nucleotide exchange factors for Rap1 and Rac1, respectively (16). An activated C3G (C3G-F; a farnesylated mutant) was also able to rescue the FA-Csk phenotype, whereas a similar farnesylated mutant of DOCK180 (DOCK180-F) failed to do so (Fig. 4B). These results suggest that activation of C3G but not DOCK180 is sufficient to complement defective signaling pathways that result from FA-Csk expression.

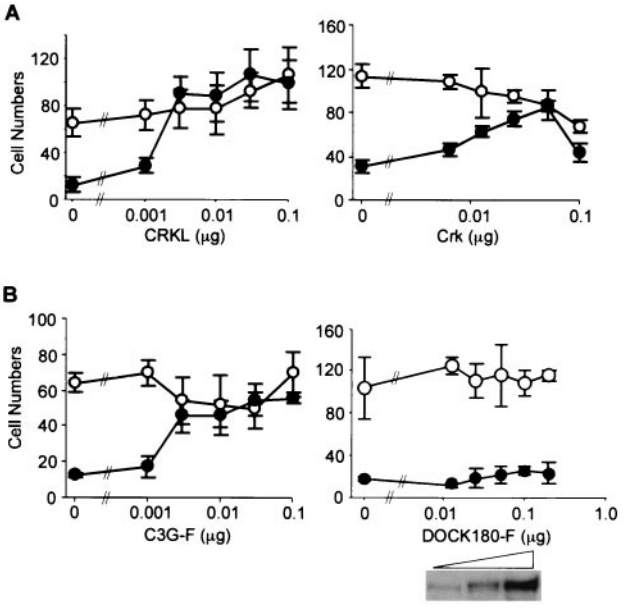

FIG. 4. CrkL/Crk and their SH3 binding protein, C3G, mediate an Src family-dependent adhesion mechanism. (A) Experiments similar to those illustrated in Fig. 3B were carried out with human CRKL or mouse Crk (cotransfection with kinase-active or -inactive CskGFP-FAT, indicated by closed or open circles, respectively). (B) Experiments similar to those described above were carried out with C3G-F or DOCK180-F (farnesylated mutant of C3G or DOCK180, respectively; Myc-tagged). The Western blot shows expression levels of DOCK180 in NIH 3T3 cells transfected with 0, 0.1, or 1 μg of plasmid in a 60-mm-diameter plate (each dose corresponds, from left to right, to 0, 0.01, and 0.1 μg of plasmid in 1 well of a 24-well plate as performed in detachment assays, respectively). In all experiments, cells were cultured for 24 h after transfection in DMEM containing 10% calf serum before fixation. The values (means ± standard deviations from a triplicate experiment) indicate the number of transfected (GFP-positive) cells remaining on the fibronectin-coated surface in 30 fields under a 25× objective in panels A and B. All experiments were repeated at least three times.

The need for Rap1 in a pathway downstream of Src. Since C3G is a guanine-nucleotide exchange factor for the small G-protein Rap1, we then determined whether activation of Rap1 rescues the FA-Csk phenotype. Indeed, an activated form of Rap1b (Rap1 12V) was able to inhibit the effect of

FIG. 3. Src activation rescues the FA-Csk phenotype. (A) Kinase-active CskGFP-FAT was electroporated into wild-type MEFs or MEFs permanently expressing SrcY529F. Wild-type MEFs showed a spherical morphology (arrows) upon expression of FA-Csk(+), while SrcY529F-expressing MEFs were resistant. Cells were stained for F-actin (red). The panel next to the photomicrographs shows an immunoblot for Src for which total cell lysates were used. (B) FA-Csk plasmid (0.1 μg of kinase-active or -inactive CskGFP-FAT, indicated by closed or open circles, respectively) was cotransfected by lipofection into NIH 3T3 cells plated on fibronectin with increasing concentrations of activated Src (Src-Y529F), its kinase-inactive variant (Src-K297M/Y529F), or normal mouse Src. (C) Cotransfection of FA-Csk plasmid (0.1 μg of kinase-active or -inactive CskGFP-LIM; closed or open circles, respectively) with increasing concentrations of CD2Fak, CD2Fak-Y397F, CasCT, or CasCT-P642A was carried out as described above. (D) Increasing concentrations of the membrane-anchored p110α subunit of phosphoinositide 3′ kinase (p110-CAAX; Myc-tagged) were cotransfected with 0.1 μg of FA-Csk plasmid per well in a 24-well plate (kinase-active or -inactive CskGFP-FAT, indicated by closed or open circles, respectively). The Western blot below panel E shows expression levels of p110α in NIH 3T3 cells transfected with 0, 0.3, or 3 μg of plasmid in a 60-mm-diameter plate (from left to right; approximately corresponding to 0, 0.03, and 0.3 μg of plasmid per well of a 24-well plate as performed in detachment assays, respectively). (E) Increasing concentrations of p210 BCR-ABL were cotransfected with 0.1 μg of FA-Csk plasmid (kinase-active or inactive CskGFP-FAT, indicated by closed or open circles, respectively) per well. In all experiments shown in panels A to E, cells were cultured for 24 h after transfection in DMEM containing 10% calf serum before fixation. The values in panels B to E (means ± standard deviations in a triplicate experiment) indicate the numbers of transfected (GFP-positive) cells remaining on the fibronectin-coated surface in 30 fields under a 25× objective. All experiments were repeated at least three times.

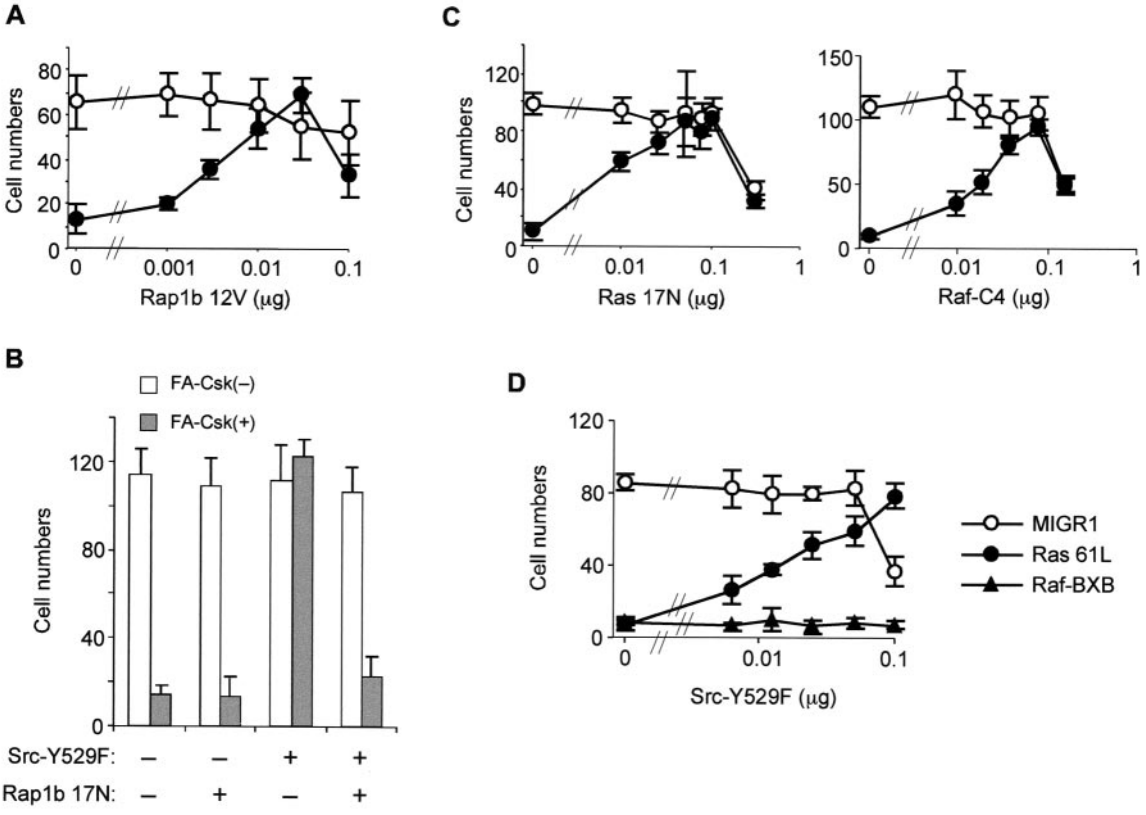

FIG. 5. Involvement of Rap1, Ras, and Raf1 in Src family-dependent adhesion. Experiments similar to those illustrated in Fig. 3B were carried out. The values (means ± standard deviations from triplicate experiments) indicate the number of transfected (GFP-positive) cells remaining on the fibronectin-coated surface in 30 fields under a 25× objective. (A) Activated Rap1 (Rap1b 12V) was cotransfected with kinase-active or -inactive CskGFP-FAT (closed or open circles, respectively) by lipofection into NIH 3T3 cells plated on fibronectin. (B) SrcY529F (0.05 μg per well) and/or a dominant-negative Rap1 (0.1 μg of Rap1b 17N) were cotransfected with FA-Csk (0.1 μg of CskGFP-FAT; kinase active or inactive) by lipofection into NIH 3T3 cells plated on fibronectin. Symbols + or − below the panel indicate the presence or absence of the transgene, respectively. (C) Increasing concentrations of a dominant negative Ras (Ras 17N) or dominant negative Raf1 (Raf-C4; the N-terminal half without the kinase domain of Raf1) were cotransfected with FA-Csk (0.1 μg of kinase-active or -inactive CskGFP-FAT, indicated by closed or open circles, respectively) into NIH 3T3 cells plated on fibronectin by lipofection. (D) A fixed amount (0.2 μg) of Ras 61L (closed circles), Raf-BXB (triangles), or empty vector control (MIGR1; open circles) was cotransfected with increasing concentrations of SrcY529F into NIH 3T3 cells plated on fibronectin-coated coverslips by lipofection. All experiments were repeated at least three times.

FA-Csk(+) (Fig. 5A). Furthermore, a dominant negative form of Rap1b (Rap1b 17N) inhibited the ability of SrcY529F to rescue the FA-Csk phenotype (Fig. 5B), thus confirming that Rap1 lies downstream of Src signaling to regulate cell-matrix adhesion. Consistent with these results, expression of Rap1b 17N at high levels by retrovirus resulted in cell rounding similar to that caused by FA-Csk(+) (data not shown).

It has been reported that Ras activation inhibits the affinity of integrins (28). We found that dominant negative forms of H-Ras and its effector Raf1 (Ras 17N and Raf-C4, respectively) were also able to rescue the cell rounding and detachment phenotype of FA-Csk(+) (Fig. 5C). Rap1 has been implicated in negative regulation of Raf1 by its interaction with the N-terminal regulatory region of Raf1 (26). A cell detachment phenotype can be induced by overexpression of activated H-Ras (Ras 61L) (38) or activated Raf1 (Raf-BXB; the C-terminal half of Raf1) (7). We found that activated Src (SrcY529F) can rescue the detachment phenotype induced by Ras 61L in a dose-dependent manner, but not that induced by Raf-BXB, consistent with the fact that Rap1 cannot inhibit this mutant Raf1 that lacks the N-terminal half including the Rap1 interaction domain (Fig. 5D). Thus, these results suggest a role for Rap1 in mediating Src signaling for regulation of integrin-mediated adhesion by counteracting the Ras pathway likely at the level of Raf1.

Affinity activation of integrins rescues the FA-Csk phenotype. The Ras-Raf1 pathway is believed to inhibit integrin affinity (27). To provide evidence that Src family-dependent pathways modulate integrin affinity, we tested the effect of the anti-β_1 integrin antibody TS2/16 that activates the conformation of human β_1 integrins and promotes β_1-mediated cell adhesion (3). We found that the TS2/16 monoclonal antibody was able to promote cell attachment and spreading of WI-38 human lung fibroblasts expressing FA-Csk(+) on a fibronectin-coated surface whereas without this antibody, FA-Csk(+) expression inhibited cell attachment and spreading on fibronectin (Fig. 6A). These results therefore suggest that FA-Csk(+) expression inhibits the affinity of the β_1 integrin subunit.

Interestingly, we noted that WI-38 cells rescued by TS2/16 showed diffuse distribution of the FA-Csk fusion protein in the

group transfected with FA-Csk(+), unlike that of FA-Csk(−) (Fig. 6B). Likewise, while integrin affinity activation by TS2/16 rescued spreading defects caused by activated Raf1 (Raf-BXB), these cells did not show FAs assessed by GFP-LIM or GFP-Pxn cotransfection (Fig. 6C; results of GFP-Pxn not shown). Therefore, it is likely that expression of FA-Csk(+) and Raf-BXB compromised the architecture of FAs. While monoclonal mouse antibodies could not be used to determine the localization of paxillin or vinculin in TS2/16 mouse monoclonal antibody-pretreated cells, our conclusion was further confirmed by localization of FA proteins Enabled and VASP using polyclonal rabbit antibodies against these proteins (20) (data not shown). Interestingly, however, the phenotypic rescue by activated Rap1 promoted localization of FA-Csk(+) to FAs (Fig. 6D). Cotransfection of CRKL and C3G-F resulted in similar rescues of the FA-Csk(+) phenotype for both spreading and FA structures (not shown). These findings therefore support the model that Rap1 activation downstream of Src kinases regulates Raf1, which otherwise inhibits not only integrin affinity but also FAs in fibroblastic cells. In agreement with these observations, our earlier experiments (Fig. 2D) also showed that kinase-active CskGFP-FAT poorly localize to FAs in cells rescued by plating on PLL, suggesting that FA structures were not formed or maintained in these cells.

In order to follow the kinetics of cell rounding and detachment, we determined the subcellular localization of FA-Csk(+) in time-lapse recordings (Fig. 7). The fusion protein accumulated to FAs at 10 h after electroporation. The cell expressing FA-Csk(+) (marked with an asterisk) at the 10-h point already showed early signs (such as retraction fibers seen in the differential interference contrast [DIC] image) of cell rounding. Between 10 and 11 h, cells lost some FA structures from the periphery (see the merged image). As shown in the enlarged image of the periphery of the cell, the loss started from the distal ends while the proximal ends were still assembled (see arrowheads in the enlarged image). These changes were specific to FA-Csk(+) and were not observed in cells expressing FA-Csk(−) [data for FA-Csk(−) not shown]. Treatment with a wide dose range of cytochalasin D did not rescue the FA-Csk(+) phenotype (not shown), thus indicating that loss of the distal end of FA structures is not due simply to a possibility of increased tension in the force-generating cytoskeleton.

The FA-Csk phenotype is independent of caspase-induced apoptosis. Since Src has been implicated in adhesion-dependent survival mechanisms (19) and in expression of the anti-apoptotic gene *Bcl-x*$_L$ (33), FA-Csk expression may cause cell death. As cell death may result in a phenotype of cell rounding and detachment, we investigated possible involvement of apoptosis in the process of cell detachment caused by FA-Csk. Caspases play a central role in executing many forms of apoptotic cell death that result from inhibition of integrin-mediated survival pathways (10, 18). Recent studies also suggest a direct link between integrins and caspases in some forms of apoptosis (8, 55). In fact, we noted that when caspase cascades are activated by subcellular targeting of the caspase domain of caspase 8 to the membrane (CD8-C [37]), NIH 3T3 cells became spherical and detached from the fibronectin-coated surface (Fig. 8A; morphological features not shown). Although rare cases of apoptosis that do not require caspase 3 may exist, it has been suggested that this caspase is essential for DNA fragmentation, chromatin condensation, and membrane blebbing in all cell types so far examined (47). Indeed, caspase 8-induced cell detachment was completely blocked by treatment with a cell-permeating inhibitor of the executioner caspase, caspase 3 (Z-DEVD-FMK; Fig. 8A). However, this inhibitor had no effect on detachment caused by FA-Csk (Fig. 8B). Although another pathway mediated by Rac1 and Ras appears to be important for adhesion-mediated survival in the absence of serum, activation of PI3K and AKT prevents detachment-induced, caspase-mediated apoptosis in the presence of serum (1, 50, 64). As expected, CD8-C expression did not lead to the detachment of NIH 3T3 cells that overexpress a myristoylated Akt mutant (Fig. 8C). On the other hand, consistent with the inability of activated PI3K p110 subunit to rescue the FA-Csk phenotype (Fig. 3E), FA-Csk effectively resulted in the detachment of these cells from fibronectin (Fig. 8D). These results therefore suggest that the primary mechanism of cell rounding and detachment caused by FA-Csk is independent of caspase-mediated apoptosis.

To provide further evidence, we examined chromosomal DNA fragmentation, the hallmark of apoptosis, by the TUNEL method in NIH 3T3 cells that express FA-Csk. To prevent cell detachment while facilitating formation of FAs at the same time (thus ensuring accumulation of FA-Csk to FAs), NIH 3T3 cells were plated onto glass coverslips coated with PLL and subsequently with fibronectin. Consistent with the observations described above, expression of kinase-active FA-Csk did not result in chromosomal DNA fragmentation (as shown by TUNEL) or apoptotic chromatin condensation (as seen in DAPI staining) at 18 h after transfection (Fig. 8E). On the other hand, FA-Csk(+)-expressing NIH 3T3 cells on fibronectin alone often show condensed nuclei and membrane blebbing suggestive of apoptosis (Fig. 2A, examined at the same time point). It has been shown that even when integrins are still occupied with ECM proteins, loss of the geometric support of cell shape induces apoptosis (12). Therefore, apoptotic cell death likely occurs secondarily to the cell rounding caused by FA-Csk expression, but it seems unlikely to be the primary cause of loss of matrix adhesion in cells expressing FA-Csk.

DISCUSSION

Csk translocates to FA structures according to the status of Src activation in embryonic fibroblasts (25). Overexpression of Csk in HeLa cells results in cell rounding accompanied by abnormal distribution of $\alpha_v\beta_5$ integrins (5). These observations prompted us to examine the physiological functions of endogenous Src family kinases by subcellular targeting of Csk to the FA protein complex. Although the cell detachment phenotype caused by inhibition of Src family kinases makes it difficult to analyze the biochemical events that parallel the cellular phenotype, we have utilized cell and molecular biology techniques to circumvent this problem. Here, we report for the first time that catalytic activity of endogenous Src family kinases is required for proper maintenance of integrin adhesive function and FAs through Rap1 activation in fibroblasts.

Overexpression of CrkL has been shown to increase integrin-mediated cell adhesion in hematopoietic cells (2). It has also been shown that CrkL, but not Crk, forms a stable com-

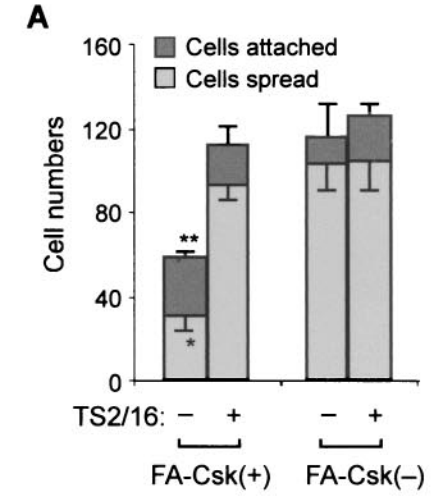
A
160
120
80
40
0
Cell numbers
Cells attached
Cells spread
**
*
TS2/16: – + – +
FA-Csk(+)
FA-Csk(–)

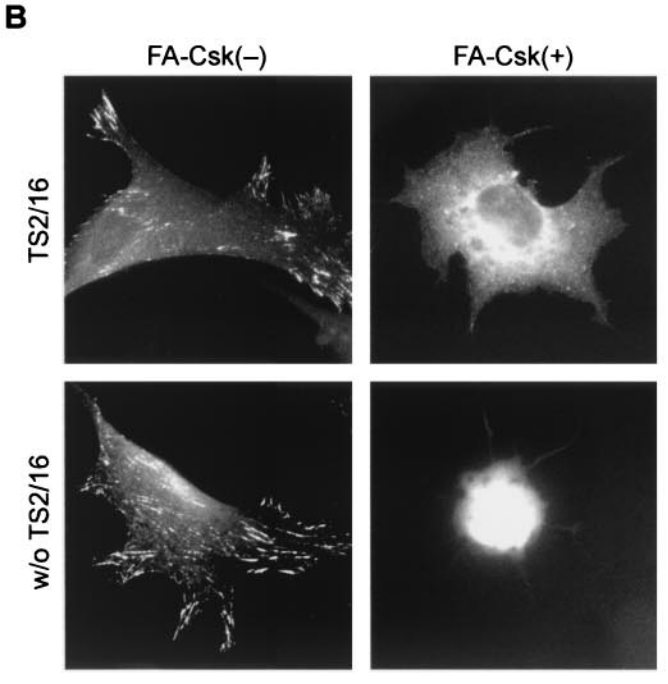
B
FA-Csk(–)
FA-Csk(+)
TS2/16
w/o TS2/16

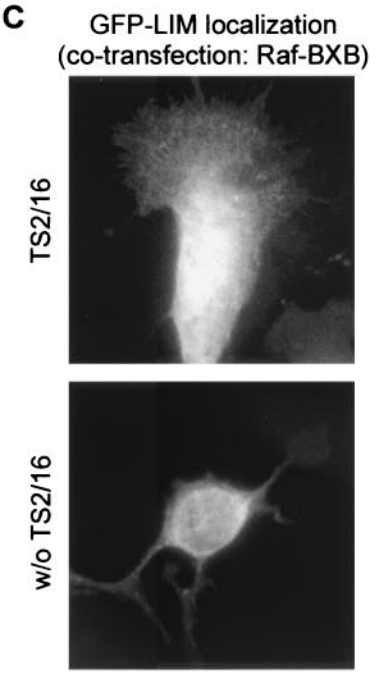
C
GFP-LIM localization
(co-transfection: Raf-BXB)
TS2/16
w/o TS2/16

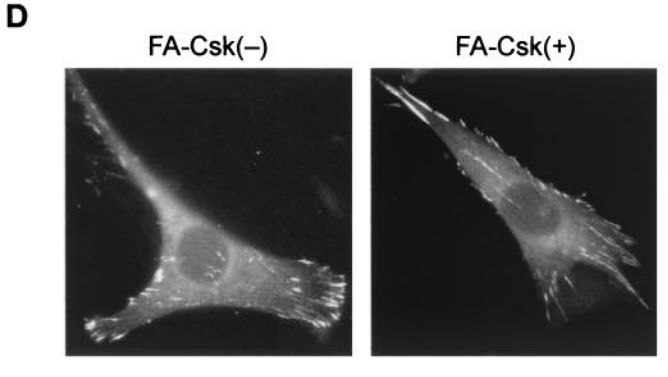
D
FA-Csk(–)
FA-Csk(+)
Co-transfection: Rap1 12V

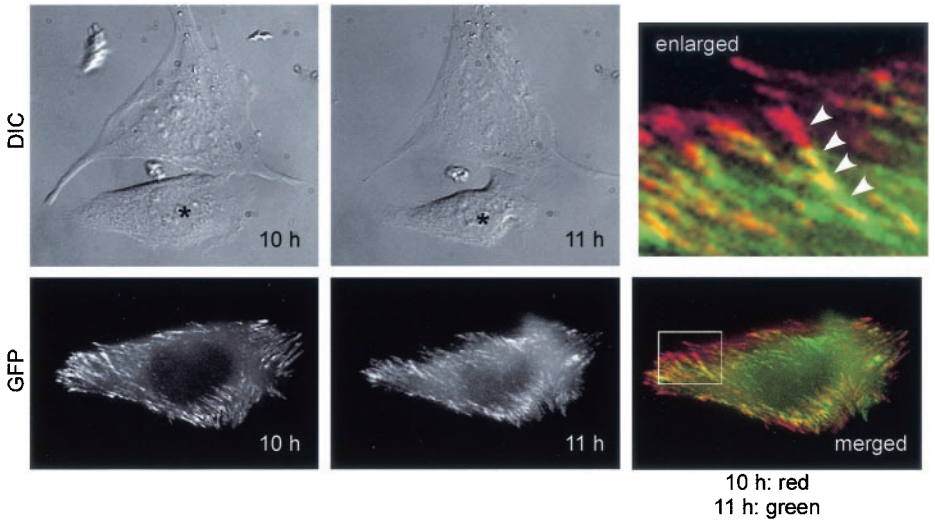

FIG. 7. Time-lapse observation of FA structures in living cells expressing kinase-active CskGFP-FAT on fibronectin. MEFs that express GFP fluorescence were observed for an extended time. DIC and GFP fluorescence images were recorded. Asterisks in the DIC images indicate an example of a GFP-positive cell. A part of the merged image (white rectangle) is enlarged to show details (enlarged). White arrowheads indicate an example of typical changes that occur in FA structures. Note that the distal part of the FA complex (red) was gone and the proximal portion of the FA complex was extended (green) between 10 and 11 h. Yellow indicates overlap in the images taken at 10 and 11 h.

plex with a Rap1 guanine-nucleotide exchange factor, C3G, in NIH 3T3 cells (15). MEFs lacking C3G cannot activate Rap1 in response to cell adhesion and show spreading defects (44). Inhibition of Rap1 by overexpression of SPA1, a Rap1GAP, in HeLa cells results in cell rounding (59). Recent studies have also implicated Rap1 in integrin-mediated adhesion in hematopoietic cells (11, 34). Rap1 is capable of activating specific effectors while it also inhibits the Ras effector Raf1 (70). Although results shown in the present study are consistent with the latter possibility, they do not exclude potential involvement of Rap1-specific effectors in Src family-dependent adhesion regulation. The signaling mechanisms of Rap1-mediated adhesion regulation have yet to be understood.

Our results suggest that the mechanisms of cell-matrix adhesion regulation by Src family-dependent activation of Rap1 cannot be explained by β_1 integrin affinity modulation alone. It has been reported that the cytoplasmic tail of α subunits contributes to adhesion regulation. Deletion of the α_4 cytoplasmic tail results in diminished integrin clustering without changing the binding affinity of $\alpha_4\beta_1$ integrins to soluble VCAM-1 (66). This clustering defect appeared to result from restricted lateral diffusion of integrins. Interestingly, *Src*$^-$ homozygous cells show abnormally strong linkage of vitronectin receptors with the cytoskeleton compared to wild-type cells or cells in which Src has been reintroduced (17), thus suggesting a role for Src in regulating the interaction of the α_v subunit with the cytoskeleton. In this regard, it is noteworthy that the N-terminal half of Src colocalizes with α_v but not β_1 integrins (17). Src family kinases and Rap1 may regulate integrin-cytoskeletal association to allow lateral diffusion for proper integrin clustering. The fact that de novo formation of FAs still occurs in cells that express FA-Csk(+), however, argues that initial integrin clustering may be normal. On the other hand, although increased integrin affinity by TS2/16 monoclonal antibody could compensate for FA-Csk(+)-induced loss of integrin-mediated adhesion, the rescued cells still failed to form stable FAs. While normal FAs had likely been formed prior to expression of FA-Csk in the time-lapse experiments, FA-Csk proteins already existed in the cell before the formation of FAs in the plating assays shown in Fig. 6. Thus, it is plausible that FA-Csk may also inhibit de novo formation of FAs. The fact that the effect of FA-Csk on cell adhesion is observed with different ECM proteins also suggests that dysfunction of integrins may not result from a mechanism specific for β_1 integrin. Failure to maintain or form proper FAs may in turn affect integrin avidity and affinity necessary for sustained cell-matrix adhesion. A role

FIG. 6. Src kinases are essential for sustained integrin activation and FA structures. (A) Effects of the β_1 integrin affinity-activating antibody TS2/16 on cell spreading in WI-38 cells expressing kinase-active or -inactive CskGFP-FAT [FA-Csk(+) or FA-Csk(−), respectively]. To prevent cell detachment while expressing FA-Csk, cells were initially transfected on PLL before TS2/16 treatment and replating. The values (means ± standard deviations) indicate the numbers of transfected (GFP-positive) cells attached (with or without spread morphology) or cells spread in 30 random fields under a 25× objective lens 1 h after replating on to fibronectin. Asterisks indicate groups significantly different from the corresponding groups without TS2/16 treatment (*t* test; *, $P < 0.001$; **, $P < 0.005$). (B) The subcellular localization of kinase-active or -inactive CskGFP-FAT [FA-Csk(+) or (−), respectively] was determined 2 h after replating with or without TS2/16 pretreatment. (C) The subcellular localization of GFP-LIM was determined in WI38 cells expressing activated Raf1 (Raf-BXB) 2 h after replating with or without TS2/16 pretreatment. WI38 cells were cotransfected with GFP-LIM and Raf-BXB as described in Materials and Methods. (D) The subcellular localization of kinase-active or -inactive CskGFP-FAT was determined in Rap1 12V-rescued NIH 3T3 cells 18 h after plating onto fibronectin. Cells were coelectroporated with 2 μg of Rap1 12V vector and 20 μg of CskGFP-FAT vector. Colocalization of paxillin with CskGFP-FAT was confirmed by immunofluorescent staining (not shown).

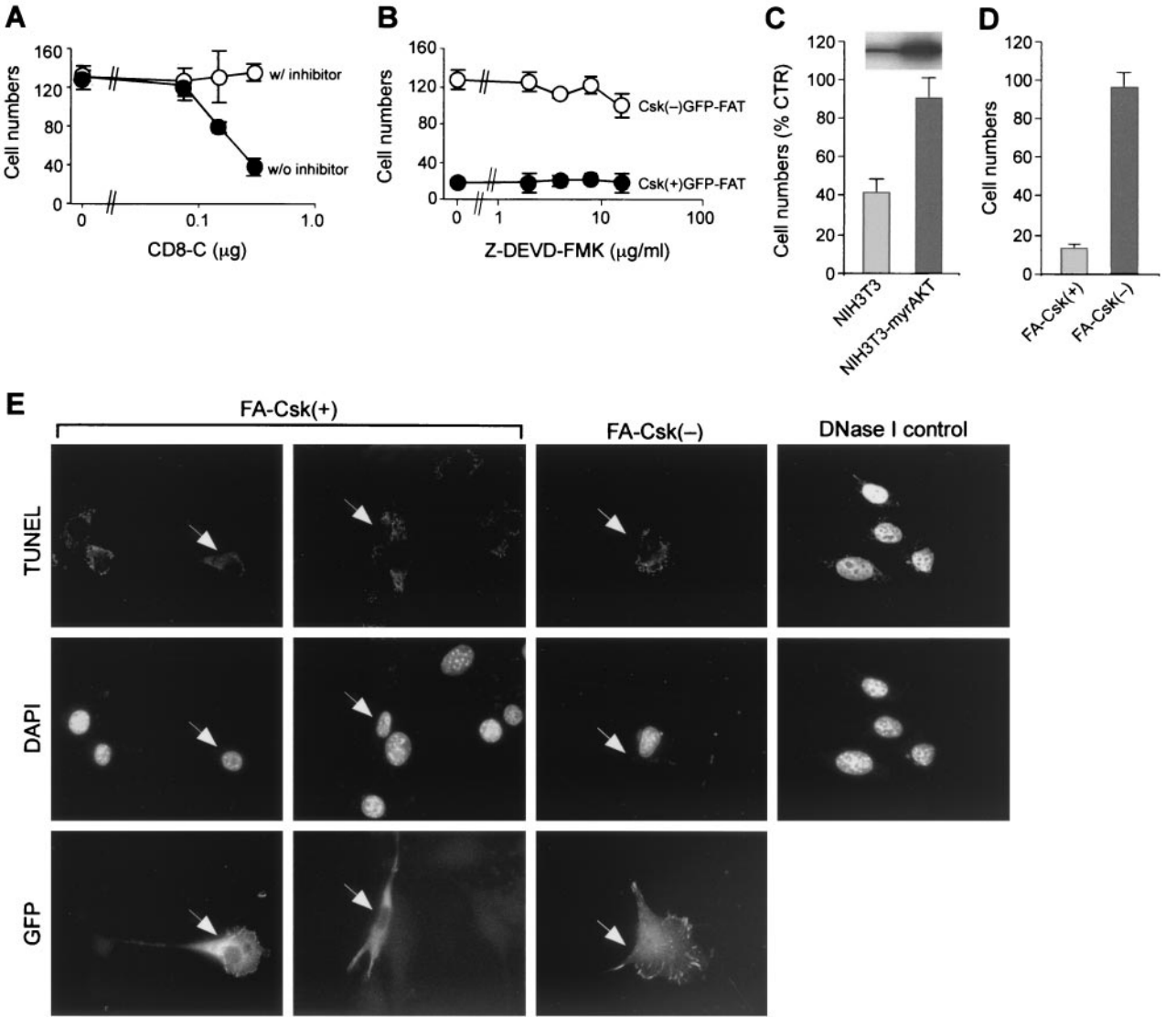

FIG. 8. The effect of FA-Csk on cell adhesion is independent of caspase-mediated apoptosis. (A) The effect of a membrane-anchored caspase domain of caspase 8 (CD8-C) on cell adhesion was determined with or without a caspase 3 inhibitor. After lipofection of NIH 3T3 cells (plated on fibronectin) with various amounts of pCEFL-CD8-C and 0.1 μg of a GFP expression plasmid, cells were cultured for 18 h with or without 8 μg of Z-DEVD-FMK (Calbiochem) per ml in DMEM containing 10% calf serum. (B) The effect of the caspase inhibitor Z-DEVD-FMK on cell detachment caused by FA-Csk(+) was determined. After lipofection of NIH 3T3 cells (plated on fibronectin) with kinase-active or inactive CskGFP-FAT, cells were cultured for 18 h in DMEM containing 10% calf serum and various doses of the caspase inhibitor. (C) Effect of activated (myristoylated) Akt on cell detachment caused by CD8-C expression. The number of GFP-positive cells remaining on coverslips in the group transfected with 0.3 μg of pCEFL-CD8-C is shown as a percentage of control (CTR) (that is, the mock-transfected group represents 100%) in parental NIH 3T3 cells as well as in those overexpressing a myristoylated mutant of Akt (NIH 3T3-myrAKT). All groups were cotransfected with a GFP expression vector. The Western blot above the bars shows the level of total Akt (endogenous and transfected) in NIH 3T3-myrAKT cells (right lane) compared to that of endogenous Akt in parental NIH 3T3 cells (left lane). (D) Effect of FA-Csk (0.1 μg of kinase-active or -inactive CskGFP-FAT plasmid) in NIH 3T3-myrAKT cells plated on fibronectin. (A to D) Values (means ± standard deviations from a triplicate experiment) indicate the numbers of transfected (GFP fluorescence-positive) cells remaining on the fibronectin-coated surface in 30 fields under a 25× objective (for panel C, values are given as percentages of control cells as noted above). (E) DNA fragmentation and chromatin condensation were determined for NIH 3T3 cells expressing FA-Csk(+) or FA-Csk(−) (kinase-active or -inactive CskGFP-FAT) plated on PLL/fibronectin double-coated coverslips 18 h after transfection. Each column shows one field of cells in three different channels (TUNEL, DAPI, and GFP signals). The arrows indicate the GFP-positive transfected cell in each group. Even after blocking endogenous biotinylated proteins, some background staining can be seen in mitochondria in TUNEL staining. The nuclei were stained with DAPI. All experiments were repeated at least three times (A to E).

for Ras and Raf1 in integrin affinity regulation has been proposed (28). Our results for FA-Csk as well as activated Raf1 suggest a complex mechanism of overall regulation of integrin adhesive functions. The precise mechanisms of integrin affinity and avidity regulation in relation to the architecture of FAs remain to be elucidated.

Src has been implicated in the activation of the Ras pathway upon growth factor and integrin stimulation (57), observations

seemingly conflicting with ours. In particular, the Ras pathway is activated by fibronectin in a manner dependent on Src in the absence of serum (54). First, a signaling pathway utilized in the absence of serum may be different from that normally used in the presence of serum (1). Second, it has been reported that Src kinases participate in at least two pathways of integrin signaling: one leads to activation of Erk through Shc-Grb2-SOS-Ras, and the other mediates Rap1 activation through Cas-Crk/CrkL-C3G (4, 63). The latter pathway appears to be important for activating the MEK-Erk pathway depending on B-Raf expression in some cells. Interestingly, activation of endogenous Src by Cas leads to activation of Rap1 but not Ras (63). Although growth factor-induced Rap1 activation does not appear to inhibit Erk in Rat-1 fibroblasts (71), B-Raf expressed in these cells likely mediates Erk activation instead of Raf1 (4). Interestingly, platelet-derived growth factor can activate Erk pathways in SYF embryonic fibroblasts (lacking all three major members of the Src family, i.e., Src, Yes, and Fyn) at lower concentrations than control cells that express Src (36). Although the precise mechanisms of this observation are unclear, one can speculate that Src family kinases participate in the regulation of Erk activation pathways. As many stimuli such as serum and growth factors activate the Ras pathway, inhibition of Src-dependent regulatory pathways by FA-Csk at FAs may lead to deregulation of Raf1 in the presence of serum or growth factors. Consistent with the ability of Rap1 to regulate Raf1, overexpression of a Rap1GAP enhances Erk phosphorylation (40). Likewise, MEFs isolated from CrkL-deficient embryos (21) show an elevated basal level of Erk phosphorylation (reported elsewhere), thus supporting our model. Nevertheless, our results do not conflict with the previous notion that Src family kinases participate in Ras activation, since FA-Csk inhibits Src kinases at FAs but not at other subcellular locations. Without proper balance of parallel Src-mediated pathways, FA structures and integrin adhesive functions may be negatively affected. The fact that low expression levels of activated Src as well as activation of endogenous Src can rescue the cell detachment phenotype of FA-Csk suggests the physiological importance of this regulatory pathway.

Although our results indicate that Src family kinases are required for integrin-mediated adhesion, the fact that MEFs lacking three major members of the Src family (SYF cells) still grow as adherent cells suggests the presence of an alternative mode of cell-matrix adhesion in these cells (36). Unlike normal cells, SYF cells may have adopted an Src family-independent mechanism by which these cells can still maintain integrin-mediated adhesion. Alternatively, it is possible that these cells retain a developmentally primitive mode of adhesion which may not require Src family kinases. *Csk*$^{-}$ mouse embryos do not show any overt defects at or earlier than embryonic day 8.5 (E8.5) (30), and embryos lacking Src, Fyn, and Yes show morphological defects at E9.5 (36). These observations suggest that embryonic cells have cellular mechanisms which do not rely on these Src family kinases in early development before E8.5 and that Src family kinases become developmentally important after midgestation. We found that although SYF cells were resistant to the effect of FA-Csk on integrin-mediated adhesion, they became sensitive when Src or Fyn was reintroduced (not shown); thus, the effect of FA-Csk is dependent on Src kinases. Although SYF cells have FA-like structures that contain vinculin (36), detailed studies of FAs have yet to be conducted. A recent study of FAs in *Src*$^{-}$ and SYF cells reported enhanced localization of tensin to FAs in these cells compared to control cells that express Src (60). Thus, SYF cells may have cell-matrix adhesion structures qualitatively different from those of normal cells. Alternatively, it is possible that acute accumulation of inactive Src kinases at FAs generated by FA-Csk may be more detrimental to FAs than the complete absence of Src family members.

Previously, Csk has been used to inhibit Src family kinases. A 10-fold or higher overexpression of Csk in HeLa cells results in cell rounding concomitant to a decrease in tyrosine phosphorylation in the cell (5). Csk overexpression by adenovirus inhibits cell spreading of astrocytes (56). To make Csk regulation of Src family kinases more efficient, the Src SH4 domain containing a myristylation signal was fused to the N terminus of Csk (14). This fusion has been analyzed for its effect on T-cell receptor signaling (14). Although a similar mutant Csk fused to the N terminus of Fyn was expressed from the *Fyn* locus in mice (31), the effect of this mutant Csk appeared to be limited to thymocytes in which Fyn is highly expressed. We found that an SH4-Csk fusion protein can produce a cell rounding phenotype in fibroblasts only at concentrations higher than that of FA-Csk, perhaps due to the limited distribution of membrane-anchored Csk to the cell-matrix adhesion apparatus (data not shown).

Subcellular targeting of the negative regulator of the Src family, Csk, to the FA complex has made it possible to investigate the functions of Src family kinases at FAs. A similar approach can be applied to studies of other signaling molecules that shuttle between the cytoplasm and FA complex. This system should be a useful tool for future investigations of such molecules.

ACKNOWLEDGMENTS

We thank A. Lin, M. Peter, and M. R. Rosner for reagents, comments, and critical reading of the manuscript; S. Bond for technical assistance at the digital microscope facility; A. H. Bouton, J. S. Brugge, S. Conzen, J. Downward, B. J. Druker, F. B. Gertler, A. Hall, J. D. Hildebrand, T. Hunter, H. Kawakatsu, B. Knudsen, A. Lin, M. Matsuda, K. Owada, W. S. Pear, E. Ruoslahti, P. J. S. Stork, S. M. Thomas, and K. Vuori for valuable reagents.

This work was supported in part by grants to A.I. from the Howard Hughes Medical Institute Research Resources Program, the Leukemia Research Foundation, the American Cancer Society Illinois Division (no. 99-04), and the American Cancer Society (RPG 00-239-01-CSM).

L.L. and M.O. contributed equally to this work.

REFERENCES

1. **Almeida, E. A., D. Ilic, Q. Han, C. R. Hauck, F. Jin, H. Kawakatsu, D. D. Schlaepfer, and C. H. Damsky.** 2000. Matrix survival signaling: from fibronectin via focal adhesion kinase to c-Jun NH(2)-terminal kinase. J. Cell Biol. **149:**741–754.
2. **Arai, A., Y. Nosaka, H. Kohsaka, N. Miyasaka, and O. Miura.** 1999. CrkL activates integrin-mediated hematopoietic cell adhesion through the guanine nucleotide exchange factor C3G. Blood **93:**3713–3722.
3. **Arroyo, A. G., A. Garcia-Pardo, and F. Sanchez-Madrid.** 1993. A high affinity conformational state on VLA integrin heterodimers induced by an anti-β1 chain monoclonal antibody. J. Biol. Chem. **268:**9863–9868.
4. **Barberis, L., K. K. Wary, G. Fiucci, F. Liu, E. Hirsch, M. Brancaccio, F. Altruda, G. Tarone, and F. G. Giancotti.** 2000. Distinct roles of the adaptor protein Shc and focal adhesion kinase in integrin signaling to ERK. J. Biol. Chem. **275:**36532–36540.
5. **Bergman, M., V. Joukov, I. Virtanen, and K. Alitalo.** 1995. Overexpressed Csk tyrosine kinase is localized in focal adhesions, causes reorganization of $\alpha_v\beta_5$ integrin, and interferes with HeLa cell spreading. Mol. Cell. Biol. **15:**711–722.

6. **Brown, M. C., J. A. Perrotta, and C. E. Turner.** 1996. Identification of LIM3 as the principal determinant of paxillin focal adhesion localization and characterization of a novel motif on paxillin directing vinculin and focal adhesion kinase binding. J. Cell Biol. **135:**1109–1123.
7. **Bruder, J. T., G. Heidecker, and U. R. Rapp.** 1992. Serum-, TPA-, and Ras-induced expression from Ap-1/Ets-driven promoters requires Raf-1 kinase. Genes Dev. **6:**545–556.
8. **Buckley, C. D., D. Pilling, N. V. Henriquez, G. Parsonage, K. Threlfall, D. Scheel-Toellner, D. L. Simmons, A. N. Akbar, J. M. Lord, and M. Salmon.** 1999. RGD peptides induce apoptosis by direct caspase-3 activation. Nature **397:**534–539.
9. **Burnham, M. R., P. J. Bruce-Staskal, M. T. Harte, C. L. Weidow, A. Ma, S. A. Weed, and A. H. Bouton.** 2000. Regulation of c-SRC activity and function by the adapter protein CAS. Mol. Cell. Biol. **20:**5865–5878.
10. **Cardone, M. H., G. S. Salvesen, C. Widmann, G. Johnson, and S. M. Frisch.** 1997. The regulation of anoikis: MEKK-1 activation requires cleavage by caspases. Cell **90:**315–323.
11. **Caron, E., A. J. Self, and A. Hall.** 2000. The GTPase Rap1 controls functional activation of macrophage integrin alphaMbeta2 by LPS and other inflammatory mediators. Curr. Biol. **10:**974–978.
12. **Chen, C. S., M. Mrksich, S. Huang, G. M. Whitesides, and D. E. Ingber.** 1997. Geometric control of cell life and death. Science **276:**1425–1428.
13. **Chen, H. C., and J. L. Guan.** 1994. Association of focal adhesion kinase with its potential substrate phosphatidylinositol 3-kinase. Proc. Natl. Acad. Sci. USA **91:**10148–10152.
14. **Chow, L. M., M. Fournel, D. Davidson, and A. Veillette.** 1993. Negative regulation of T-cell receptor signalling by tyrosine protein kinase p50^{csk}. Nature **365:**156–160.
15. **de Jong, R., A. van Wijk, N. Heisterkamp, and J. Groffen.** 1998. C3G is tyrosine-phosphorylated after integrin-mediated cell adhesion in normal but not in Bcr/Abl expressing cells. Oncogene **17:**2805–2810.
16. **Feller, S. M., G. Posern, J. Voss, C. Kardinal, D. Sakkab, J. Zheng, and B. S. Knudsen.** 1998. Physiological signals and oncogenesis mediated through Crk family adapter proteins. J. Cell. Physiol. **177:**535–552.
17. **Felsenfeld, D. P., P. L. Schwartzberg, A. Venegas, R. Tse, and M. P. Sheetz.** 1999. Selective regulation of integrin-cytoskeleton interactions by the tyrosine kinase Src. Nat. Cell Biol. **1:**200–206.
18. **Frisch, S. M., and R. A. Screaton.** 2001. Anoikis mechanisms. Curr. Opin. Cell Biol. **13:**555–562.
19. **Frisch, S. M., K. Vuori, E. Ruoslahti, and P. Y. Chan-Hui.** 1996. Control of adhesion-dependent cell survival by focal adhesion kinase. J. Cell Biol. **134:**793–799.
20. **Gertler, F. B., K. Niebuhr, M. Reinhard, J. Wehland, and P. Soriano.** 1996. Mena, a relative of VASP and Drosophila Enabled, is implicated in the control of microfilament dynamics. Cell **87:**227–239.
21. **Guris, D. L., J. Fantes, D. Tara, B. J. Druker, and A. Imamoto.** 2001. Mice lacking the homologue of the human 22q11.2 gene *CRKL* phenocopy neurocristopathies of DiGeorge syndrome. Nat. Genet. **27:**293–298.
22. **Hasegawa, H., E. Kiyokawa, S. Tanaka, K. Nagashima, N. Gotoh, M. Shibuya, T. Kurata, and M. Matsuda.** 1996. DOCK180, a major CRK-binding protein, alters cell morphology upon translocation to the cell membrane. Mol. Cell. Biol. **16:**1770–1776.
23. **Henderson, B. R.** 2000. Nuclear-cytoplasmic shuttling of APC regulates β-catenin subcellular localization and turnover. Nat. Cell Biol. **2:**653–660.
24. **Hildebrand, J. D., M. D. Schaller, and J. T. Parsons.** 1993. Identification of sequences required for the efficient localization of the focal adhesion kinase, pp125^{FAK}, to cellular focal adhesions. J. Cell Biol. **123:**993–1005.
25. **Howell, B. W., and J. A. Cooper.** 1994. Csk suppression of Src involves movement of Csk to sites of Src activity. Mol. Cell. Biol. **14:**5402–5411.
26. **Hu, C. D., K. Kariya, T. Okada, X. Qi, C. Song, and T. Kataoka.** 1999. Effect of phosphorylation on activities of Rap1A to interact with Raf-1 and to suppress Ras-dependent Raf-1 activation. J. Biol. Chem. **274:**48–51.
27. **Hughes, P. E., and M. Pfaff.** 1998. Integrin affinity modulation. Trends Cell Biol. **8:**359–364.
28. **Hughes, P. E., M. W. Renshaw, M. Pfaff, J. Forsyth, V. M. Keivens, M. A. Schwartz, and M. H. Ginsberg.** 1997. Suppression of integrin activation: a novel function of a Ras/Raf-initiated MAP kinase pathway. Cell **88:**521–530.
29. **Hynes, R. O.** 1992. Integrins: versatility, modulation, and signaling in cell adhesion. Cell **69:**11–25.
30. **Imamoto, A., and P. Soriano.** 1993. Disruption of the *csk* gene, encoding a negative regulator of Src family tyrosine kinases, leads to neural tube defects and embryonic lethality in mice. Cell **73:**1117–1124.
31. **Kanazawa, S., D. Ilic, M. Hashiyama, M. Okada, T. Noumura, S. Aizawa, and T. Suda.** 1996. Impaired development of CD4+ CD8+ thymoctes by csk-'knock-in' into fyn locus. Oncogene **13:**199–204.
32. **Kaplan, K. B., J. R. Swedlow, D. O. Morgan, and H. E. Varmus.** 1995. c-Src enhances the spreading of *src*$^{-}$ $^{-}$ fibroblasts on fibronectin by a kinase-independent mechanism. Genes Dev. **9:**1505–1517.
33. **Karni, R., R. Jove, and A. Levitzki.** 1999. Inhibition of pp60$^{c\text{-}Src}$ reduces *Bcl-XL* expression and reverses the transformed phenotype of cells overexpressing EGF and HER-2 receptors. Oncogene **18:**4654–4662.
34. **Katagiri, K., M. Hattori, N. Minato, S. Irie, K. Takatsu, and T. Kinashi.** 2000. Rap1 is a potent activation signal for leukocyte function-associated antigen 1 distinct from protein kinase C and phosphatidylinositol-3-OH kinase. Mol. Cell. Biol. **20:**1956–1969.
35. **Kawakatsu, H., T. Sakai, Y. Takagaki, Y. Shinoda, M. Saito, M. K. Owada, and J. Yano.** 1996. A new monoclonal antibody which selectively recognizes the active form of Src tyrosine kinase. J. Biol. Chem. **271:**5680–5685.
36. **Klinghoffer, R. A., C. Sachsenmaier, J. A. Cooper, and P. Soriano.** 1999. Src family kinases are required for integrin but not PDGFR signal transduction. EMBO J. **18:**2459–2471.
37. **Martin, D. A., R. M. Siegel, L. Zheng, and M. J. Lenardo.** 1998. Membrane oligomerization and cleavage activates the caspase-8 (FLICE/MACHalpha1) death signal. J. Biol. Chem. **273:**4345–4349.
38. **Minden, A., A. Lin, F. X. Claret, A. Abo, and M. Karin.** 1995. Selective activation of the JNK signaling cascade and c-Jun transcriptional activity by the small GTPases Rac and Cdc42Hs. Cell **81:**1147–1157.
39. **Miyamoto, S., H. Teramoto, O. A. Coso, J. S. Gutkind, P. D. Burbelo, S. K. Akiyama, and K. M. Yamada.** 1995. Integrin function: molecular hierarchies of cytoskeletal and signaling molecules. J. Cell Biol. **131:**791–805.
40. **Mochizuki, N., Y. Ohba, E. Kiyokawa, T. Kurata, T. Murakami, T. Ozaki, A. Kitabatake, K. Nagashima, and M. Matsuda.** 1999. Activation of the ERK/MAPK pathway by an isoform of rap1GAP associated with G alpha(i). Nature **400:**891–894.
41. **Moran, T. J., S. Gray, C. A. Mikosz, and S. D. Conzen.** 2000. The glucocorticoid receptor mediates a survival signal in human mammary epithelial cells. Cancer Res. **60:**867–872.
42. **Nada, S., M. Okada, A. MacAuley, J. A. Cooper, and H. Nakagawa.** 1991. Cloning of a complementary DNA for a protein-tyrosine kinase that specifically phosphorylates a negative regulatory site of p60$^{c\text{-}src}$. Nature **351:**69–72.
43. **Nakamoto, T., R. Sakai, K. Ozawa, Y. Yazaki, and H. Hirai.** 1996. Direct binding of C-terminal region of p130^{Cas} to SH2 and SH3 domains of Src kinase. J. Biol. Chem. **271:**8959–8965.
44. **Ohba, Y., K. Ikuta, A. Ogura, J. Matsuda, N. Mochizuki, K. Nagashima, K. Kurokawa, B. J. Mayer, K. Maki, J. Miyazaki Ji, and M. Matsuda.** 2001. Requirement for C3G-dependent Rap1 activation for cell adhesion and embryogenesis. EMBO J. **20:**3333–3341.
45. **Pear, W. S., J. P. Miller, L. Xu, J. C. Pui, B. Soffer, R. C. Quackenbush, A. M. Pendergast, R. Bronson, J. C. Aster, M. L. Scott, and D. Baltimore.** 1998. Efficient and rapid induction of a chronic myelogenous leukemia-like myeloproliferative disease in mice receiving P210 bcr/abl-transduced bone marrow. Blood **92:**3780–3792.
46. **Plattner, R., L. Kadlec, K. A. De Mali, A. Kazlauskas, and A. M. Pendergast.** 1999. c-Abl is activated by growth factors and Src family kinases and has a role in the cellular response to PDGF. Genes Dev. **13:**2400–2411.
47. **Porter, A. G., and R. U. Jänicke.** 1999. Emerging roles of caspase-3 in apoptosis. Cell Death Differ. **6:**99–104.
48. **Rao, M. S., and D. J. Anderson.** 1997. Immortalization and controlled in vitro differentiation of murine multipotent neural crest stem cells. J. Neurobiol. **32:**722–746.
49. **Richardson, A., R. K. Malik, J. D. Hildebrand, and J. T. Parsons.** 1997. Inhibition of cell spreading by expression of the C-terminal domain of focal adhesion kinase (FAK) is rescued by coexpression of Src or catalytically inactive FAK: a role for paxillin tyrosine phosphorylation. Mol. Cell. Biol. **17:**6906–6914.
50. **Rytomaa, M., K. Lehmann, and J. Downward.** 2000. Matrix detachment induces caspase-dependent cytochrome c release from mitochondria: inhibition by PKB/Akt but not Raf signalling. Oncogene **19:**4461–4468.
51. **Sabe, H., A. Hata, M. Okada, H. Nakagawa, and H. Hanafusa.** 1994. Analysis of the binding of the Src homology 2 domain of Csk to tyrosine-phosphorylated proteins in the suppression and mitotic activation of c-Src. Proc. Natl. Acad. Sci. USA **91:**3984–3988.
52. **Schaller, M. D.** 1999. Complex formation with focal adhesion kinase: a mechanism to regulate activity and subcellular localization of Src kinases. Mol. Biol. Cell **10:**3489–3505.
53. **Schaller, M. D., J. D. Hildebrand, J. D. Shannon, J. W. Fox, R. R. Vines, and J. T. Parsons.** 1994. Autophosphorylation of the focal adhesion kinase, pp125^{FAK}, directs SH2-dependent binding of pp60^{src}. Mol. Cell. Biol. **14:**1680–1688.
54. **Schlaepfer, D. D., M. A. Broome, and T. Hunter.** 1997. Fibronectin-stimulated signaling from a focal adhesion kinase-c-Src complex: involvement of the Grb2, p130cas, and Nck adaptor proteins. Mol. Cell. Biol. **17:**1702–1713.
55. **Stupack, D. G., X. S. Puente, S. Boutsaboualoy, C. M. Storgard, and D. A. Cheresh.** 2001. Apoptosis of adherent cells by recruitment of caspase-8 to unligated integrins. J. Cell Biol. **155:**459–470.
56. **Takayama, Y., S. Tanaka, K. Nagai, and M. Okada.** 1999. Adenovirus-mediated overexpression of C-terminal Src kinase (Csk) in type I astrocytes interferes with cell spreading and attachment to fibronectin. Correlation with tyrosine phosphorylations of paxillin and FAK. J. Biol. Chem. **274:**2291–2297.
57. **Thomas, S. M., and J. S. Brugge.** 1997. Cellular functions regulated by Src family kinases. Annu. Rev. Cell Dev. Biol. **13:**513–609.
58. **Thomas, S. M., P. Soriano, and A. Imamoto.** 1995. Specific and redundant roles of Src and Fyn in organizing the cytoskeleton. Nature **376:**267–271.

59. **Tsukamoto, N., M. Hattori, H. Yang, J. L. Bos, and N. Minato.** 1999. Rap1 GTPase-activating protein SPA-1 negatively regulates cell adhesion. J. Biol. Chem. **274:**18463–18469.
60. **Volberg, T., L. Romer, E. Zamir, and B. Geiger.** 2001. pp60(c-src) and related tyrosine kinases: a role in the assembly and reorganization of matrix adhesions. J. Cell Sci. **114:**2279–2289.
61. **Vuori, K., H. Hirai, S. Aizawa, and E. Ruoslahti.** 1996. Introduction of p130^{cas} signaling complex formation upon integrin-mediated cell adhesion: a role for Src family kinases. Mol. Cell. Biol. **16:**2606–2613.
62. **Wennstrom, S., and J. Downward.** 1999. Role of phosphoinositide 3-kinase in activation of Ras and mitogen-activated protein kinase by epidermal growth factor. Mol. Cell. Biol. **19:**4279–4288.
63. **Xing, L., C. Ge, R. Zeltser, G. Maskevitch, B. J. Mayer, and K. Alexandropoulos.** 2000. c-Src signaling induced by the adapters Sin and Cas is mediated by Rap1 GTPase. Mol. Cell. Biol. **20:**7363–7377.
64. **Xiong, W., and J. T. Parsons.** 1997. Induction of apoptosis after expression of PYK2, a tyrosine kinase structurally related to focal adhesion kinase. J. Cell Biol. **139:**529–539.
65. **Xu, W., A. Doshi, M. Lei, M. J. Eck, and S. C. Harrison.** 1999. Crystal structures of c-Src reveal features of its autoinhibitory mechanism. Mol. Cell **3:**629–638.
66. **Yauch, R. L., D. P. Felsenfeld, S. K. Kraeft, L. B. Chen, M. P. Sheetz, and M. E. Hemler.** 1997. Mutational evidence for control of cell adhesion through integrin diffusion/clustering, independent of ligand binding. J. Exp. Med. **186:**1347–1355.
67. **Zernicka-Goetz, M., J. Pines, K. Ryan, K. R. Siemering, J. Haseloff, M. J. Evans, and J. B. Gurdon.** 1996. An indelible lineage marker for Xenopus using a mutated green fluorescent protein. Development **122:**3719–3724.
68. **Zhang, Z., K. Vuori, H. Wang, J. C. Reed, and E. Ruoslahti.** 1996. Integrin activation by R-ras. Cell **85:**61–69.
69. **Zolotukhin, S., M. Potter, W. W. Hauswirth, J. Guy, and N. Muzyczka.** 1996. A "humanized" green fluorescent protein cDNA adapted for high-level expression in mammalian cells. J. Virol. **70:**4646–4654.
70. **Zwartkruis, F. J., and J. L. Bos.** 1999. Ras and Rap1: two highly related small GTPases with distinct function. Exp. Cell Res. **253:**157–165.
71. **Zwartkruis, F. J., R. M. Wolthuis, N. M. Nabben, B. Franke, and J. L. Bos.** 1998. Extracellular signal-regulated activation of Rap1 fails to interfere in Ras effector signalling. EMBO J. **17:**5905–5912.